EUROREGIO BNAM2022
Joint Acoustics Conference
9th-11th of May, Aalborg, Denmark

Simple dynamic measurement system for testing IMU sensor precision in spatial audio

Petar Franček[1,*], Kristian Jambrošić[1], Marko Horvat[1], Vedran Planinec[1]

[1]Department of Electroacoustics, Faculty of Electrical Engineering and Computing, University of Zagreb, Croatia.

*petar.francek@fer.hr

Abstract
Spatial sound is used in a variety of systems these days. The application of high-quality audio systems with real-time processing ranges from hi-fi systems to systems for live sound and virtual reality. The data needed to (re)create realistic surround sound audio is often collected using Inertial Measurement Unit (IMU) sensors. With technological progress, the number of such sensors in many devices is constantly increasing. By combining the data from all sensor devices, a dynamic virtual audio field can be created that provides an immersive experience for the user. When processing the collected raw data, attention must be paid to the precision and tolerance of the sensors. The IMU sensors used in this type of measurement usually consist of an accelerometer, a gyroscope and sometimes a magnetometer, all of which are triaxial. When processing and editing the measured data, the effects of low precision and accuracy, parameter drift and latency can greatly affect the measurement uncertainty and the overall user experience. Sensor devices used for spatial audio fall into three groups: VR headsets, smartphones and DIY sensor systems. However, the cost of a device does not necessarily guarantee the accuracy of the measured data.

This paper presents the results of dynamic measurements on sensors used in embedded systems. Several different types of sensors with different shapes and sizes are used. Some are built on PCB boards with processing units, while others are implemented as modules on dedicated PCBs. A microcontroller is used for data processing. The most widely used open-source platform Arduino is used for the measurements. To avoid the magnetic influence of the moving parts in the setup, a simple aluminium/plastic pendulum is used. To minimise the measurement error, all measurements are taken simultaneously. The measurement results are compared, and the quality of the measured sensors is evaluated.

Keywords: IMU sensor accuracy, binaural synthesis, spatial audio

1 Introduction

Nowadays, devices capable of processing and determining its own orientation are used by many people on a daily basis. These types of devices, e.g. smartphones, cameras, wristbands, trinkets, etc., often consist of a microcontroller for processing purposes and an Inertial Measurement Unit (IMU) sensor for determining their orientation. The usage of this type of devices is growing rapidly, resulting in an increasing number of features built into the devices for optimal user experience and, at the same time, maximizing its utilization. This paper presents the results of measurements conducted on such devices as part of the research focused on determining whether such hardware can be used for binaural synthesis. The data from IMU sensors consist of accelerometer and gyroscope sensor output generated during the measurements. All measurements were taken simultaneously to minimise measurement error, and to facilitate direct comparison of measurement results.
Two previous publications authored by this research team report the results of static and dynamic measurements performed on various smartphones and Arduino microcontrollers. In [1], the focus was put on testing the static performance of the devices, i.e., their stability and resilience to drift of the measured

parameters. In [2], the same devices were investigated in dynamic conditions, i.e. they were placed on turntables with constant angular speed and the same set of measurements was performed. The goal of the research presented in this paper is to investigate the behaviour of these devices in a different, but still controlled dynamic conditions to determine whether their quality is sufficient for use in auralization.

2 Methodology

During the design of the measurement setup, extra attention was paid to minimizing any kind of disturbing magnetic field close to the device under test (DUT). This setup is used for measuring the accelerometer, gyroscope and magnetometer quality of DIY sensors, smartphones and VR sets as a part of the AUTAURA research project [3]. The design of this setup proved to be a comprehensive task, as it had to facilitate dynamic measurements with variable speeds of moving parts, while avoiding the use of any kind of devices that generate magnetic fields. Forces needed for the dynamic measurements can be generated using electrical motors (with interference on magnetic field) or by using other types of actuators (compressed air, etc.). Both of solutions have complexity and cost of a design exceed limitations of a project resources. The optimal solution that meets these specific demands was a setup that utilizes a simple mathematical pendulum (gravity pendulum). Similar solutions have been implemented in [4, 5]. An example of a gravity pendulum is shown in Figure 1.

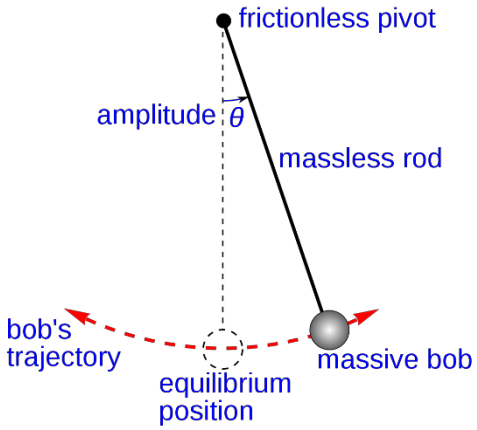

Figure 1: A simple gravity pendulum [6].

Besides minimizing the disturbance caused by magnetic fields, there are several other benefits that come from using a pendulum. It is quite easy to determine the starting parameters (e.g. the height of the bob, the maximum deflection angle θ) and to calculate the force that causes the pendulum to swing back and forth, passing through its equilibrium position. The force F that acts on the bob perpendicular to the rod is expressed as:

$$F = -mg \sin\theta \tag{1}$$

where m represents the centre of mass, g is the gravity constant, and θ with its maximum deflection angle of the pendulum represents starting position. This force is linear to the sensor readings of one accelerometer axis. The period of mathematical oscillation T is constant and can be determined as (2):

$$T = 2\pi\sqrt{\frac{l}{g}} \tag{2}$$

where l represents the length of the pendulum. It can be observed that the period T depends only on the length of the rod (or thread) and the gravity constant. On the other hand, mass m and angle θ have no influence on the period of the pendulum.
Extra consideration was given to the comparability of measured results. It is important to note that the measurements were conducted using three different types of microcontrollers that have been obtained as a project resource for these measurements. That means that the internal clocks in the controllers could exhibit a mismatch during measurements. The process of calibration has been designed with the assumption that the processing of the same set of instructions consumes the same amount of time for each microcontroller [7]. All the devices (microcontrollers with sensors) were left in operating condition for a long period of time, i.e. much longer than the duration of the actual measurements (48+ hours compared to 30 seconds). The time base data was extrapolated by calculating the input parameters. In addition, the use of three different microcontrollers with different hardware and software setups led to different initialization times on each microcontroller-sensor combination. To overcome the problem of inconsistent starting time of sensors, a pushbutton switch was installed. Each microcontroller/sensor has a different booting and warmup time. After powering up and finishing the boot/warmup sequence, time synchronization was done by activating the pushbutton. The code is executed outside of the continuous loop in the microcontroller, thus removing any effect on speed or load on microprocessor [8]. This approach solves the problem of inconsistent internal clocks of each microcontroller and their internal time.
To determine the latency of the sensors, a specific approach is used. A microcontroller with an LED display is used only to display time in the millisecond range, while other microcontrollers are used to perform sensor measurements at the same time. A high-speed video camera [9] is positioned in the equilibrium position, i.e. the lowest point of the pendulum, where the velocity of the pendulum reaches its highest values. Using the recorded high-speed video, it is easy to determine the position of the pendulum where the forces and the velocity are at their maximum. The timestamp can be recorded by reading the display on the recorded video. Using the calibration described above, the latency between the time where the values of measured sensor data reach their maximum, and the timestamp logged with camera can be calculated.

3 Measurement setup

The pendulum was assembled using aluminium, plastic, and wooden parts to minimize its influence on the magnetic field and to lower the mass of the pendulum. A 3-meter-long aluminium rod with a thin cross-section was suspended from the ceiling by means of a small steel axle, which forces the pendulum to swing in a single plane. The rotational friction that appears during the movement of the pendulum (and its axle) was minimized using high-class ball bearings. At the other end of the aluminium rod, a wooden plate is fixed to the rod as the bob, i.e. the moving mass. To increase this mass, a steel counterweight is fixed to the plate as well. The surface of the wooden plate is used to mount the sensor devices with Arduino microcontrollers. Figure 2 shows the measurement setup used in this research, with the pendulum at its maximum displacement from equilibrium. Pictures of setup are taken with loudspeakers positioned behind pendulum, but measurements were conducted without presence of loudspeakers.
The pendulum was made as long as physically possible and its length was limited by the ceiling height of 3.2 m, in order to maximize the period of the motion and the generated forces during measurements. The pendulum moves along the axis (swings on the axle) stretching in the east-west direction, thus restricting its movement to the north-south direction. A set of six microcontrollers and IMU sensors is located on the wooden plate. There are three types of microcontrollers and four different sensor modules. The wooden plate with mounted microcontrollers and sensors is displayed in Figure 3.
One microcontroller is dedicated to displaying the elapsed time with millisecond precision, two microcontrollers have built-in IMU sensors, and three microcontrollers have external connected IMU PCBs. Microcontrollers and sensors are mounted from north to south and labelled as follows: display, LSM6DS3 (external sensor module), NanoInt (internal), UnoInt (internal), ICMAK (external), and DOFv2 (external). The labels correspond to their IMU sensor chip, respectively: LSM6DS3 [10], LSM9DS1 [11], LSM6DS3 [10], ICM-20600 [12], and MPU-9250 [13]. In Figure 3 it is easy to identify the order and the position of each

device. Extra effort was made to position the sensor chips on the marked axis, thus assuring direct comparability of all measured results.
The orientation of the sensor chips is determined by their position on the PCB. The mounting points of the PCBs are used to fix the sensors in the position where minimal wiring to electrical modules is needed. The minimal wiring setup of all sensors mounted on the wooden plate means that power supply is directly connected to sensors, and communication cables are directly connected from each sensor to specific microcontroller. This setup also be seen in Figure 3. In these positions, the sensor modules output the data according to the orientation of axes shown in Figure 4.

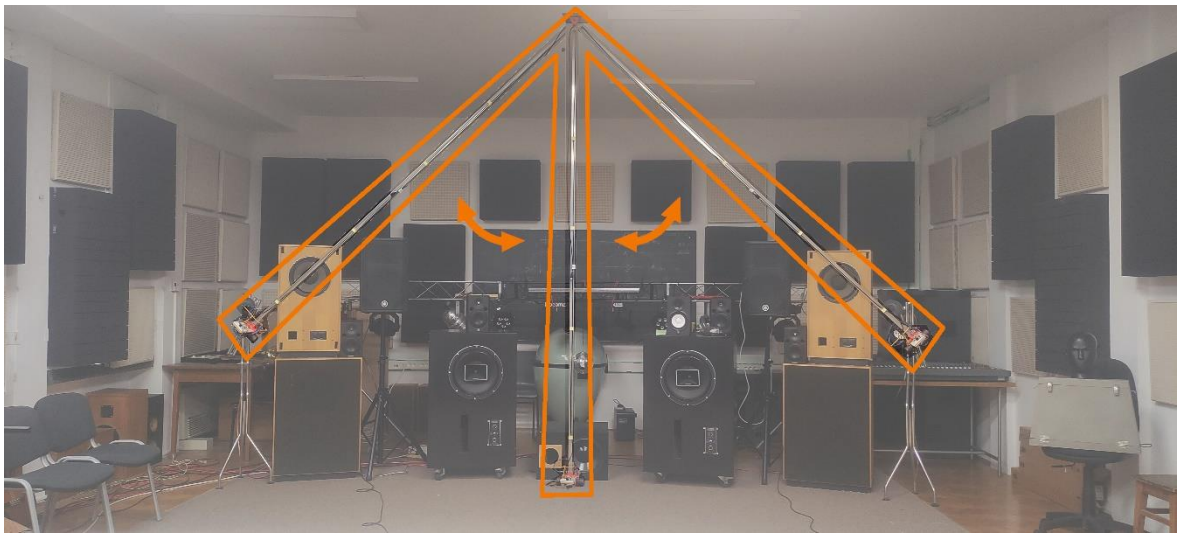

Figure 2: Measurement setup based on a pendulum, with maximum displacement positions on both sides and the equilibrium position.

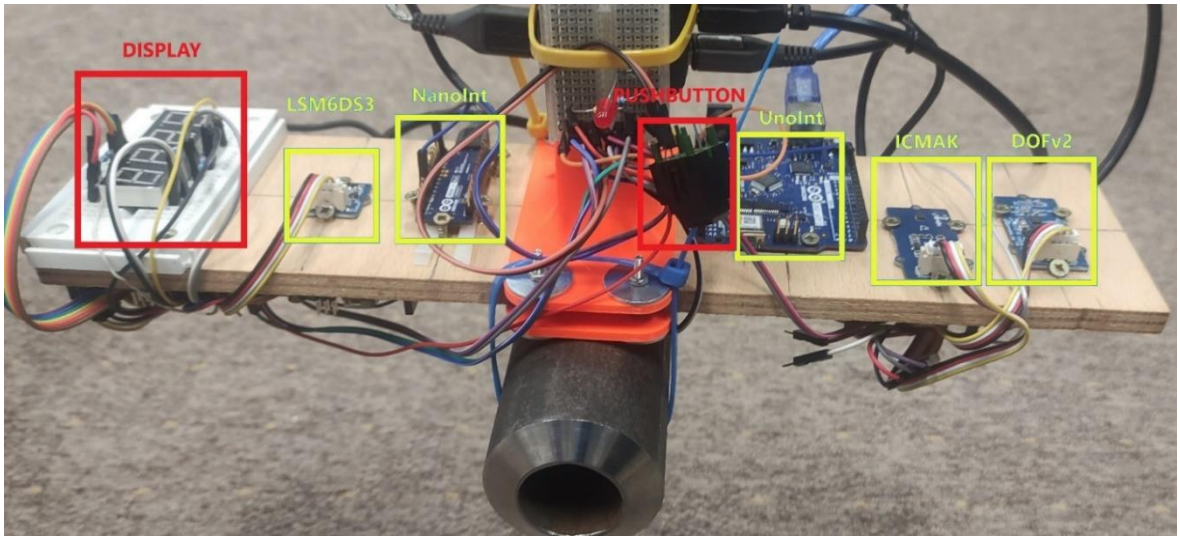

Figure 3: Wooden plate with mounted microcontrollers and sensor modules.

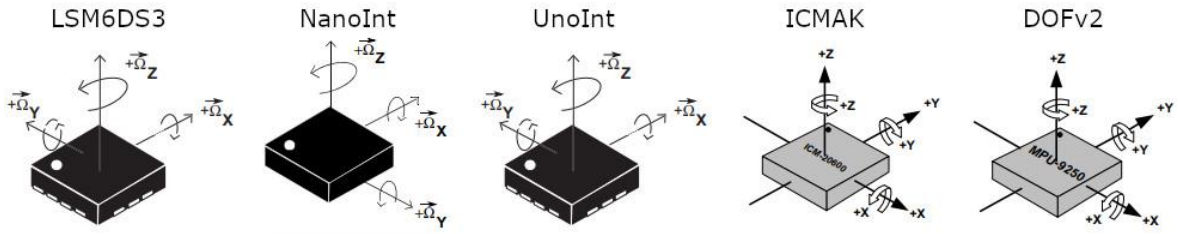

Figure 4: The orientation of the axes for the investigated sensors [10-13].

The orientation of the DOFv2 is used as a reference. All other sensor data was processed with reference to the orientation of this sensor. The mismatch of the axes of different sensors can be seen in Figure 4.
Used setup has hardware limitations. The built-in IMU sensors are connected to the processing unit using two different protocols. In particular, the NanoInt uses the I2C protocol, while the UnoInt uses the SPI protocol. These connections are determined and cannot be changed. As no significant difference in the sensor communication time was observed, the authors decided to use the I2C protocol for all other sensors.
The measured data include the internal time of the microprocessor, the accelerometer data, and the gyroscope data. The magnetometer data was recorded as well during the measurements, and it will be analysed and published as the comparison of IMU magnetometer data obtained from DIY sensors, smartphones, VRs and other sensing devices. The microprocessor internal time is used to avoid latency in communication between the microcontrollers and the data storage system. The lack of the microprocessor RTC module is also justified by minimizing microprocessor load, so that the highest possible sample rate of a IMU sensor can be achieved. Each microprocessor is optimized for a specific task, i.e. to read and send sensor data without any additional computation.
In this setup stock libraries from sensor manufacturers were and parameters (if there is any) for highest refresh rate and precision were selected.

4 Results

This section displays the results of the conducted measurements. All the measurements were performed simultaneously using six microcontrollers. Several sets of measurements were made for different starting height (deflection angle) of the pendulum. T1 and T2 parameters were determined using readings from a record of a high-speed camera video in lowest position of a pendulum where acceleration of Z axis and angular speed of X axis has its maximum. Using this parameters latency of each sensor is calculated. It is possible to observe T1 and T2 as a red vertical line in Figure 6 and Figure 8 around T=4 sec and T=38 sec. For a very precise and accurate comparison, pre-processing of measured data is done. The calibration described above is followed by normalization of the measured data.

4.1 Calibration and normalization of data

The calibration process ensures that the starting and the ending moment of the measurement are aligned in time for all microcontrollers and sensor combinations. The effect of calibration can be observed using graphical representation of the measured data. Without calibration, the data coming from different DUTs neither start nor end at the same moment in time because of different internal clocks of processing units. The time differences with and without calibration are shown on the left chart in Figure 5.

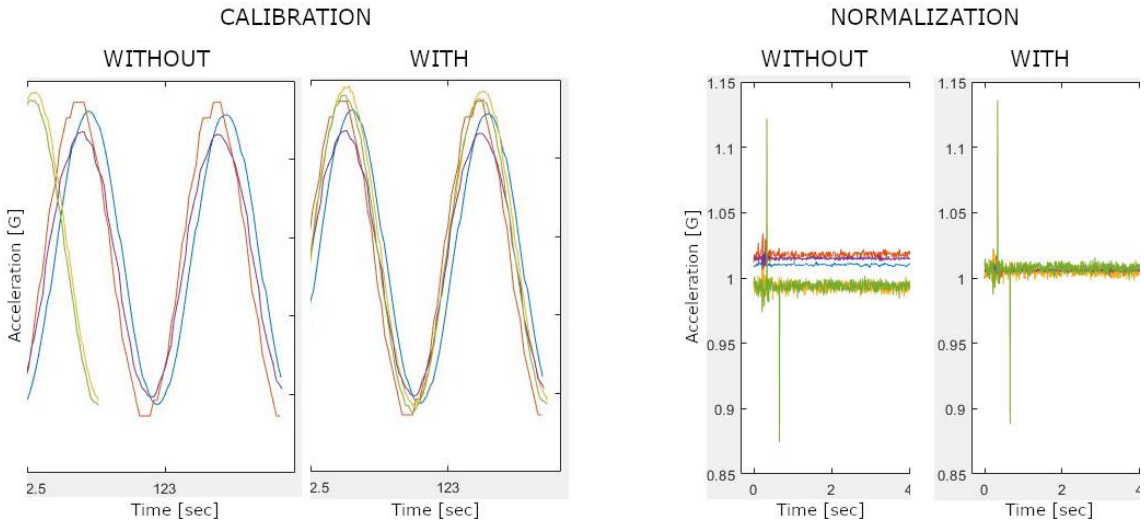

Figure 5: Comparison of measured data with and without pre-processing: left – calibration, right – normalization.

The goal of the normalization procedure is to align the amplitude of raw sensor data obtained from different DUTs. For example, stable static sensors readings of accelerometers without drift are in range from 0.99 to 1.02G. To overcome this difference during the comparison of results, process of normalization is used. The result of normalization is displayed on the right chart in Figure 5.
The described pre-processing applied on measured data facilitates the direct comparison of different DUTs and makes all subsequent calculations much simpler. Nevertheless, all raw data has been saved in a unique database for further calculations and manipulation.

4.2 The results of acceleration measurements

The first measured parameter to be presented is acceleration. It was measured with X axis pointing to the west, Y axis to the south, and Z axis to the floor. The results of acceleration measurements are visible in Figure 6.

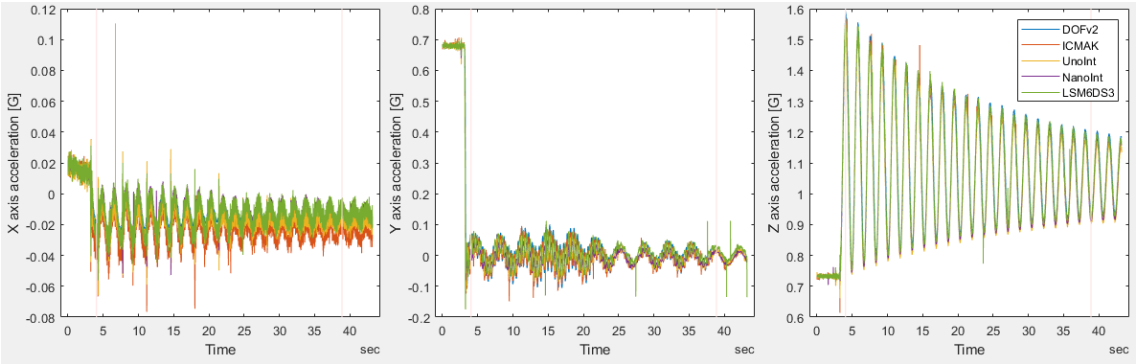

Figure 6: Acceleration results for three axes.

As expected, the biggest amplitudes are found for the Z axis, while on other axes the acceleration values are much lower, but still present. By zooming in on one part of the chart that shows the acceleration on the X axis, it is noticeable that the measured signal of NanoInt and LSM6DS3 is, in fact, out of phase compared to the signals obtained from DOFv2, ICMAK and UnoInt. Figure 7 shows this behaviour.

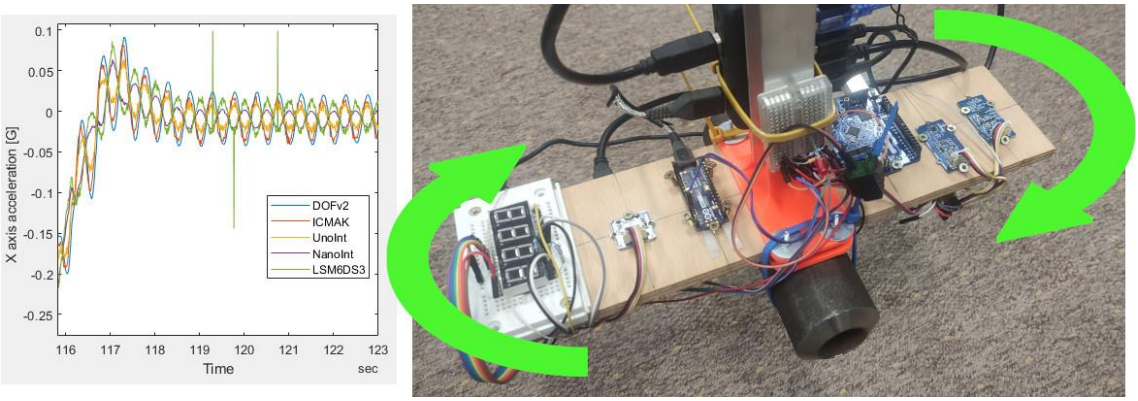

Figure 7: Opposite acceleration forces on X axis in period of harmonic axial rotation.

On the left side of Figure 7 (until timestamp 117 sec) it is possible to observe that all five sensor measurements have a negative acceleration and same trend. From 117 sec onwards, the direction of oscillations of LSM6DS3 and UnoInt sensor are opposite from the direction of the remaining sensors. On the right side of Figure 7, green arrows indicate the rotation direction of the measurement setup (from west to north), thus revealing the reason for such behaviour. The same effect was observed in the data for all three acceleration axes. Table 1 shows the numerical results of the measured parameters with maximum values for Z axis of setup and latency calculated using values T1 and T2 from video record.

Table 1: Numerical representation of recorded acceleration data for Z axis.

Parameter	LSM6DS3	NanoInt	UnoInt	ICMAK	DOFv2
Amplitude (T1) [mG]	1565.80	1557.40	1549.55	1574.05	1591.01
Amplitude (T2) [mG]	914.81	910.39	902.05	905.05	928.11
Latency (T1) [ms]	32.5	38.0	5.3	0.5	22.0
Latency (T2) [ms]	43.0	49.0	28.0	1.0	32.5

It can be noted that in this measurement, ICMAK is a sensor with lowest latency.

4.3 The results of gyroscope measurements

The gyroscope data was recorded during the same measurements as the data obtained for the acceleration. As expected, the maximum amplitude of the angular velocity was found for the rotation along the X axis. As a consequence of torsional forces, the frequency for the other two axes is much higher due to a significantly shorter radius of oscillation. Figure 8 shows the raw data obtained from gyroscope measurements for all three axes.

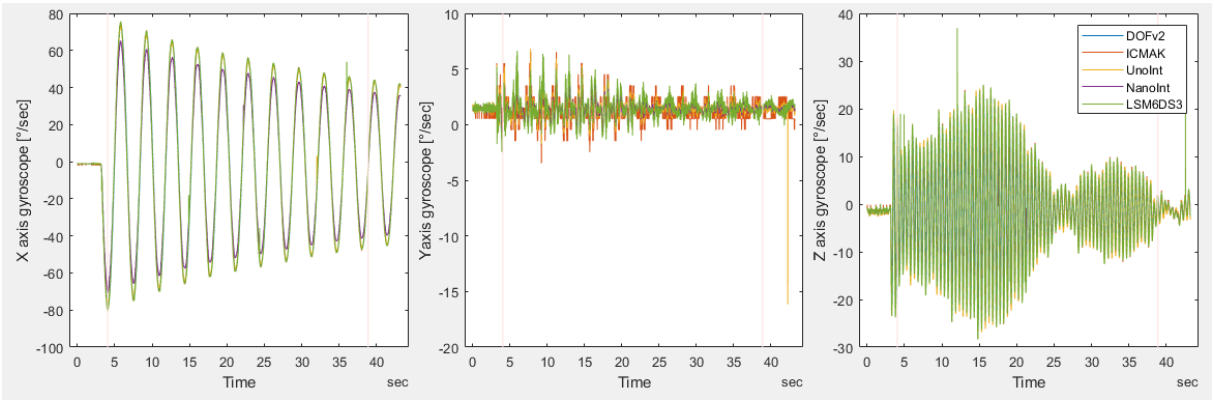

Figure 8: Gyroscope results for three axes.

In this case, the torsion of the wooden plate does not affect sensor readings as it does for the accelerometer data, i.e. in this case no out-of-phase readings have been observed. All rotations are in the same direction, as expected. Values for Y and Z axis are as expected different from 0 because of a torsion movement explained in right part of a Figure 7. Table 2 shows the numerical results of the measured gyroscope parameters for the X axis.

Table 2: Numerical representation of recorded gyroscope data for X axis.

Parameter	LSM6DS3	NanoInt	UnoInt	ICMAK	DOFv2
Amplitude (T1) [°/sec]	80.79	71.06	78.39	80.02	78.91
Amplitude (T2) [°/sec]	44.16	37.58	42.98	43.98	43.28
Latency (T1) [ms]	5.5	6.0	5.3	0.5	33.9
Latency (T2) [ms]	9.8	7.5	16.0	1.0	41.5

5 Conclusions

The described process of investigating the quality of the IMU sensors has raised research questions that must be highlighted and addressed. First of all, this setup has mentioned hardware limitations. The built-in IMU sensors are connected to the processing unit using two different protocols and the authors decided to use the I2C protocol for all sensors where it was possible.

It is important to mention that in some cases the NanoInt sensor had the data refresh status register at false state, although the values were changing, and new ones were updated. This problem was solved by not checking the state of the status register and simply reading the values from it.

The lack of high precision in some sensors can be the consequence of hardware limitations and/or suboptimal software implementations. In our examples where stock libraries were used, and problems were detected when the processing speed was compared with alternative libraries written by the community. Some community-written libraries enabled a quadruple increase in speed, and improved precision. The problem with such types of stock libraries is that the code is often undocumented and without any references, so the accuracy of the received data might be questionable.

One of the sensors does not have direction marks on its PCB nor any marks on the chip, so its true orientation was ambiguous. Things get more complex when community forums are contacted, because the marks on the PCB are not consistent for the accelerometer and the gyroscope. After rethinking and checking the datasheet, an agreement was reached regarding the orientation of the sensor based on common sense. The data obtained from the conducted measurements confirmed that the selected directions/orientations were properly chosen.

The process of calibrating the time base of each microcontroller can be omitted by recording the data directly in real time. This approach requires more hardware resources, and it can be used in real time processing. It was not implemented as a solution to be examined in this paper because the authors wanted to record data in the microcontroller, thus avoiding the unnecessary additional lag and uncertainty that stem from communication between the microprocessor and the data storage unit.

The results of measurements show that the ICMAK module exhibits the lowest latency. On the other hand, that same module also has the lowest resolution. The best resolution and the highest latency were found for the DOFv2 module. The features of the optimal device are the result of a compromise between responsiveness (as low latency as possible) and resolution (as high as possible).

Further measurements of sensors built into smartphones and VRs or implemented in some other ways are planned in the future using the same pendulum setup. Upon finishing all measurements, a comparison with representative samples of each group will be done to assess the quality of different devices and their usability in binaural head-tracking systems.

Acknowledgements

The authors acknowledge financial support by the Croatian Science Foundation, (HRZZ IP-2018-01-6308, "Audio Technologies in Virtual Reality Systems for Auralization Applications (AUTAURA)".

References

[1] Kristian Jambrošić, Miljenko Krhen, Marko Horvat and Tomislav Jagušt. and Peter Aspinall. Measurement of IMU sensor quality used for head tracking in auralization systems. *Proceedings of e-Forum Acusticum 2020*, December 2020.

[2] Kristian Jambrošić, Vedran Planinec, Marko Horvat and Petar Franček. Precision of inertial measurement unit sensors in head-tracking systems used for binaural synthesis. *INTER-NOISE and NOISE-CON Congress and Conference Proceedings, pp. 2634-2645(12),* August 2021. doi: 10.3397/IN-2021-2190.

[3] [Online, Accessed 03/03/2022], https://autaura.fer.hr/autaura

[4] S. E. R. Charel, E. H. Binugroho, M. A. Rosyidi, R. S. Dewanto and D. Pramadihanto. Kalman filter for angle estimation using dual inertial measurement units on unicycle robot. *2016 International Electronics Symposium (IES),* 2016

[5] Kee-Young Choi, Se-Ah Jang, Yong-Ho Kim. Calibration of Inertial Measurement Units Using Pendulum Motion. *International Journal of Aeronautical and Space Sciences, 11(3), pp. 234-239*, 2010. doi: 10.5139/IJASS.2010.11.3.234

[6] [Online, Accessed 03/03/2022], https://en.wikipedia.org/wiki/Pendulum

[7] Bruce Jacob, Spencer W. Ng and David T. Wang. Memory Systems, Cache, DRAM, Disk. *Elsevier Inc., 2008*, doi: 10.1016/B978-0-12-379751-3.X5001-2

[8] [Online, Accessed 04/03/2022], https://www.arduino.cc/reference/en/language/structure/sketch/loop/

[9] [Online, Accessed 04/03/2022], https://www.samsung.com/global/galaxy/what-is/frames-per-second/

[10] [Online, Accessed 08/03/2022], https://botland.store/index.php?controller=attachment&id_attachment=1307

[11] [Online, Accessed 08/03/2022], https://www.st.com/resource/en/datasheet/lsm9ds1.pdf

[12] [Online, Accessed 09/03/2022], https://3cfeqx1hf82y3xcoull08ihx-wpengine.netdna-ssl.com/wp-content/uploads/2021/05/DS-000184-ICM-20600-v1.1.pdf

[13] [Online, Accessed 10/03/2022], https://invensense.tdk.com/wp-content/uploads/2015/02/MPU-9250-Datasheet.pdf?ref_disty=digikey